LAWRENCE
LIVERMORE
NATIONAL
LABORATORY

LLNL-JRNL-509671

Dislocation dynamics simulation of Frank-Read sources in anisotropic alpha-Fe

S. P. Fitzgerald, S. Aubry, S. L. Dudarev, W. Cai

October 31, 2011

Modelling and Simulation in Materials Science and Engineering

Disclaimer

Dislocation Dynamics Simulation of Frank-Read Sources in anisotropic α-Fe

S.P. Fitzgerald[1], S. Aubry[2,3], S.L. Dudarev[1] and W. Cai[2]

[1] *EURATOM/CCFE Fusion Association, Culham Science Centre, Abingdon UK OX14 3DB*
[2] *Department of Mechanical Engineering, Stanford University, CA, USA*
[3] *Lawrence Livermore National Laboratory, Livermore, CA 94550, USA*

Abstract

Frank-Read sources are among the most important examples of dislocation sources in crystals, and their operation facilitates dislocation multiplication and hence yield and plastic flow. Iron is known to become highly elastically-anisotropic as the $\alpha - \gamma$ transition at 912℃ is approached, a temperature regime of critical importance for emerging technologies such as fusion and next-generation fission reactors. Using dislocation dynamics simulations based on anisotropic linear elasticity theory, we show that the isotropic elastic approximation leads to large errors in the activation stress of Frank-Read sources in iron at high temperatures. The critical stresses obtained from anisotropic elasticity are very different from the isotropic calculations and vary significantly between orientations. In particular, the increased variation of the dislocation energy with orientation leads to certain source configurations becoming operational at very low applied stresses, a result which is incompatible with isotropic elasticity, and is consistent with the very low yield stresses observed experimentally in α-Fe at high temperatures.

Key words: anisotropic elasticity, dislocation dynamics, yield strength, Frank-Read sources, alpha-Iron.

1 Introduction

In three dimensions, the linear elastic behavior of a crystal with cubic symmetry can be encoded by three independent parameters, for example the elastic moduli C_{12}, C_{44} and $C' = (C_{11} - C_{12})/2$, where C_{12} describes the relation between normal stress and strain components, and C_{44}, C' are two independent shear moduli. If the crystal is assumed to be isotropic, the two shear moduli coincide, and the mathematical machinery required to perform calculations

is greatly simplified, particularly where dislocations are concerned [1]. As a result of this improved tractability, the vast majority of the existing literature on elasticity-based simulation of dislocations utilizes the isotropic approximation (see for example [2, 3, 4] and references therein). However, most crystals are elastically anisotropic to some extent, and for the technologically important case of iron the anisotropy ratio $A = C_{44}/C'$ reaches almost 8 as the temperature approaches that of the $\alpha - \gamma$ transition at 912℃ [5]. If we wish to study the elastic and plastic behavior of, for example, ferritic and martensitic steels for advanced nuclear fission and fusion applications, the isotropic approximation to elasticity theory does not apply.

In this paper, we report dislocation dynamics (DD) simulations of one of the most important features of microstructure in metals: the Frank-Read (FR) source [6]. By allowing dislocations to multiply, these sources, amongst other mechanisms, give rise to yield and plastic flow. The empirical elastic moduli we use [5] correspond to iron at 900℃, a regime of great importance for nuclear technology, and one where the anisotropy of the lattice plays a dominant rôle.

In the next section we turn our attention to the FR source itself, and develop an algorithm to define and compute the critical stress required to initiate dislocation multiplication for various configurations of source, in each of the four principal slip systems in the body-centered-cubic (bcc) lattice. Next we present our results, and compare them with those obtained from DD simulations using Voigt- and Reuss-averaged isotropic elastic moduli, and from an analytical line tension model. We also discuss the shapes adopted by the sources as they bow out, and explain the unusual cusped configurations we observe in terms of the thermodynamic instability of certain dislocation orientations in highly anisotropic bcc crystals [7, 8]. The critical stress, and the behavior very close to criticality, varies significantly across the FR source configurations we consider, and differs both qualitatively and quantitatively from the isotropic approximations.

2 Simulation Methodology

Our code is based on an extension of the DD simulation package `ParaDiS`[9] to account for anisotropic elasticity [10, 11]. The dislocation structure is discretized, represented by a network of nodes connected by straight segments.

A FR source [6] starts out as a segment of dislocation line pinned between two points. The pinning can be caused by interactions with other dislocations, impurities or precipitates. Under an appropriate applied stress the segment will bow out, increasing the elastic energy stored in the crystal, leading to a stressed equilibrium configuration. Once a critical stress (defined below) is ex-

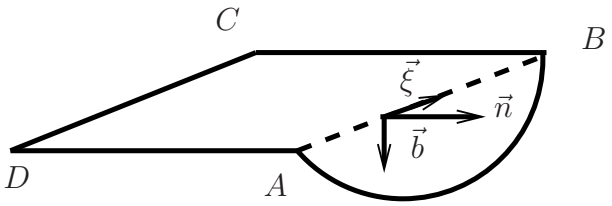

Fig. 1. Dislocation configuration. Segments BC, DC and DA are fixed. Only nodes inside segment AB are allowed to move, with nodes A and B fixed too. The glide plane of segment AB is perpendicular to the plane of rectangle $ABCD$. Initially, AB is a straight segment and $|AD|$ is four times $|AB|$.

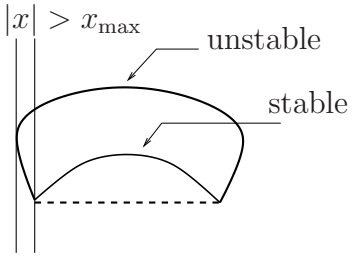

Fig. 2. Criteria for determining the dislocation stability: when $x_{\max}$ is reached, the dislocation is defined as unstable; when the maximum velocity of the nodes is lower than $10^{-5}\mathring{A}/s$, the dislocation is stable.

ceeded, the bowed-out segment becomes unstable, and there no longer exists an equilibrium configuration. The segment loops back on itself, whence sections annihilate and pinch off. This results in a dislocation shear loop, which may continue to expand, and a fresh pinned segment, which may begin the process again. This mechanism in principle allows unlimited plastic displacement, provided the stress is gradually increased above the critical threshold (in practice, the expanding loops are likely to encounter obstacles, which may lead to the formation of pile-ups [12, 13]). The critical stresses for various configurations of FR sources will be intimately related to the yield stress of the crystal, and their calculation is hence of interest.

The initial dislocation configuration in our simulations is a rectangle with three sides that are fixed, see Fig. 1. The stress field acting on each dislocation segment due to the rest of the loop is calculated by summing contributions from every segment (including itself), using for each an expression for the field due to an isolated finite segment [10, 11]. Because the stress field of a finite dislocation segment is not unique, we add three segments to the Frank-Read segment AB to form a closed loop. The segments BC, CD and DA are defined to be sessile so that we can focus on the behavior of the source segment AB under stress. As the stress increases, the dislocation bows out in the plane orthogonal to $ABCD$.

In order to numerically define the critical stress, we have to choose a criterion for dislocation stability in DD simulations. As the applied stress increases,

the dislocation starts to bow out and its line length increases. The dislocation becomes unstable when the line normal to the initial segment is crossed, as shown in Fig. 2. Numerically, this happens whenthe lateral excursion of the line exceeds $x_{\max}$. This definition should not depend on $x_{\max}$ provided $x_{\max}$ is large enough. We used two different values of $x_{\max}$ of $1.5\,x_0$ and $1.7\,x_0$, where x_0 is the initial dislocation length, and the predicted critical stress remains the same. When a dislocation reaches a stable configuration under an applied stress, its velocity vanishes. We compute the maximum velocity on the dislocation nodes, and choose the criterion that if this is less than $10^{-5}\mathring{A}/s$, the dislocation is stable.These two criteria ensure that the values of the critical stress for all Frank-Read configurations are computed consistently.

3 Results

We determine the critical stress required to operate FR sources in ten configurations occurring in the bcc lattice: an initial edge and an initial screw orientation for each of the four principal bcc slip systems, namely [100](001), [100](011), $\frac{1}{2}[111](0\bar{1}1)$, $\frac{1}{2}[111](11\bar{2})$, plus two additional $\boldsymbol{b} = [100]$ mixed configurations which will be discussed later. The different cases studied are summarized in Table 1. At fixed initial length $L = 1000\,a_0$, where a_0 is the lattice constant, we study how the shape of the dislocation and its critical stress vary as a function of its initial Burgers vector, line direction and glide plane. In these simulations, the values of the elastic constants are $C_{11} = 122$GPa, $C_{12} = 99$GPa and $C_{44} = 13.3$GPa, corresponding to α-Fe at 900℃ [5]. The core cut-off parameter is equal to the norm of the Burgers vector $\boldsymbol{b}$. Effective isotropic moduli were calculated using both Voigt ($\mu \approx 64$GPa and $\nu = 0.29$) and Reuss ($\mu \approx 27$GPa and $\nu = 0.40$) averages. (See [10] for a detailed discussion of the various isotropic averaging procedures).

3.1 Dislocation shapes after bow out

The shapes of the dislocations just below the critical stress are shown in Fig. 3. For cases 5-10, we have added a core energy to smooth out the dislocation shapes as discussed in [10]. Firstly, in all cases the shape assumed by the bowing dislocation is very different from the smooth oval shapes predicted by isotropic elasticity. Sharp corners in agreement with those predicted by previous studies are observed [8, 14], and the bowing segments approximately describe segments of the equilibrium curves for the shear loops studied in [10]. Particularly in the $\boldsymbol{b} = [100]$ cases, the sharp corners effectively allow the expanding sources to avoid high energy dislocation orientations, so the expansion is achieved without the requirement to generate these (see Fig. 3). This is

Table 1
Eight Frank-Read sources corresponding to an initial screw and edge segment in each of the four principle bcc slip systems (cases 1-8) plus two $\boldsymbol{b} = [100]$ mixed configurations (see text). Burgers vector $\boldsymbol{b}$, glide plane normal $\boldsymbol{n}$ and line direction $\boldsymbol{\xi}$.

Case	$\boldsymbol{b}$	$\boldsymbol{n}$	initial $\boldsymbol{\xi}$	character
1	$[100]$	$[011]$	$\frac{1}{\sqrt{2}}[01\bar{1}]$	edge
2	$[100]$	$[011]$	$[100]$	screw
3	$[100]$	$[001]$	$[0\bar{1}0]$	edge
4	$[100]$	$[001]$	$[100]$	screw
5	$\frac{1}{2}[111]$	$[01\bar{1}]$	$\frac{1}{\sqrt{6}}[\bar{2}11]$	edge
6	$\frac{1}{2}[111]$	$[01\bar{1}]$	$\frac{1}{\sqrt{3}}[111]$	screw
7	$\frac{1}{2}[111]$	$[11\bar{2}]$	$\frac{1}{\sqrt{2}}[\bar{1}10]$	edge
8	$\frac{1}{2}[111]$	$[11\bar{2}]$	$\frac{1}{\sqrt{3}}[111]$	screw
9	$[100]$	$[011]$	$\frac{1}{\sqrt{3}}[11\bar{1}]$	mixed
10	$[100]$	$[001]$	$\frac{1}{\sqrt{2}}[110]$	mixed

unlike the case where the crystal is isotropic, or only mildly anisotropic, when sharp corners cannot develop since they are not stable minimizers of the elastic energy. The emergenvce of these thermodynamically-unstable orientations are characteristic of large elastic anisotropy[7, 8]. It should be noted that, once the critical stress is reached, no equilibrium solution exists and system becomes essentially dynamic in nature. However, the self force which acts to orient the segments in the lowest energy directions [14] still operates, and the sharp corners remain on moving dislocations in our DD simulations..

The $\boldsymbol{b} = [100]$ cases 1,2 and 3,4 are fairly symmetric between the initial edge and screw cases, particularly for 1,2. This is because the lowest energy configurations actually lie in mixed orientations [8], and the bow-out proceeds via the extension of the segment along these directions. The opposite is true for cases 5,6 and 7,8 where $\boldsymbol{b} = \frac{1}{2}[111]$. At high anisotropy, the $\frac{1}{2}[111]$ screw becomes very low energy, and the FR sources which start as a pinned edge can easily expand by extending dislocation segments along screw directions. The FR sources which begin as a pinned screw, however, must generate higher energy edge segments in order to expand, and the shapes they adopt reflect this screw-edge asymmetry.

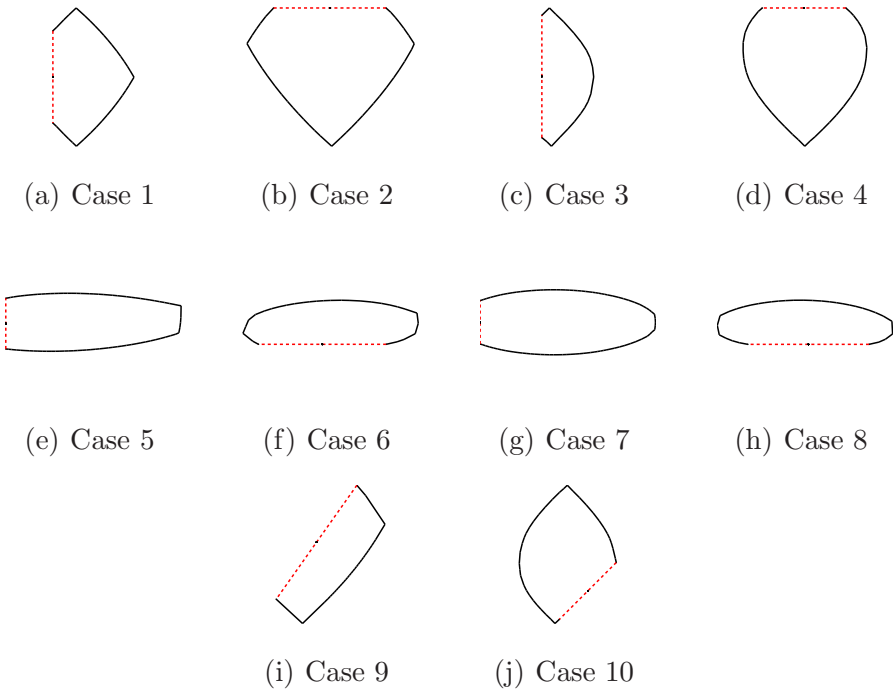

(a) Case 1 (b) Case 2 (c) Case 3 (d) Case 4

(e) Case 5 (f) Case 6 (g) Case 7 (h) Case 8

(i) Case 9 (j) Case 10

Fig. 3. Shape of Frank-Read sources just below the critical stress.

3.2 Critical stresses

We computed the critical stress for the configurations defined in Table 1 using isotropic and anisotropic elasticity, using both `ParaDiS` and an analytical anisotropic line tension model. The results are shown in Fig. 4, with the definition that the (scalar) critical stress is the constant σ such that

$$\hat{\boldsymbol{\sigma}} = \sigma \left(\frac{\boldsymbol{b}}{|\boldsymbol{b}|} \otimes \frac{\boldsymbol{n}}{|\boldsymbol{n}|} + \frac{\boldsymbol{n}}{|\boldsymbol{n}|} \otimes \frac{\boldsymbol{b}}{|\boldsymbol{b}|} \right),$$

with $\boldsymbol{b}$ the Burgers' vector and $\boldsymbol{n}$ the glide plane normal vector. This allows the dimensional scalar magnitude σ to be separated from the geometry-dependent tensorial part of the stress. Firstly consider the isotropic results in Fig. 4(a). The critical stress required to activate these FR sources is fairly uniform across the orientations, and scales $\sim \mu|\boldsymbol{b}|/L$ where L is the initial length of the pinned segment, $\boldsymbol{b}$ is the Burgers' vector and μ the shear modulus Cases 1–4 are shifted slightly higher relative to cases 5–8 simply because $|[100]| > |\frac{1}{2}[111]|$. The sources which are initially pinned in the edge orientation (2,4,6,8) have a lower critical stress than the screws (1,3,5,7) since to operate they must generate screw segments, which are always lower energy in an isotropic crystal.

The situation is markedly different in the anisotropic case, which is characterized by a much larger variation across the orientations: a factor of four between the lowest and highest critical stresses as seen in Fig. 4(b). Several

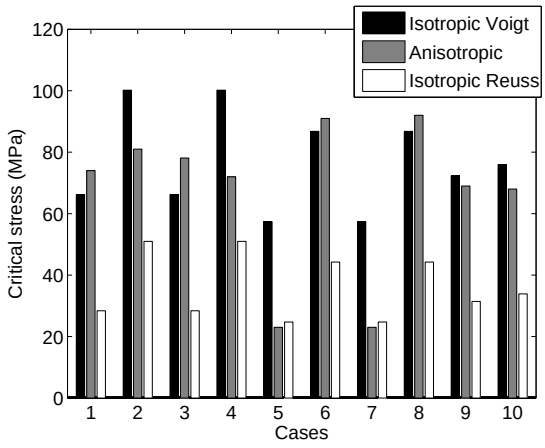

(a) Comparison for $L = 1000\, a_0$

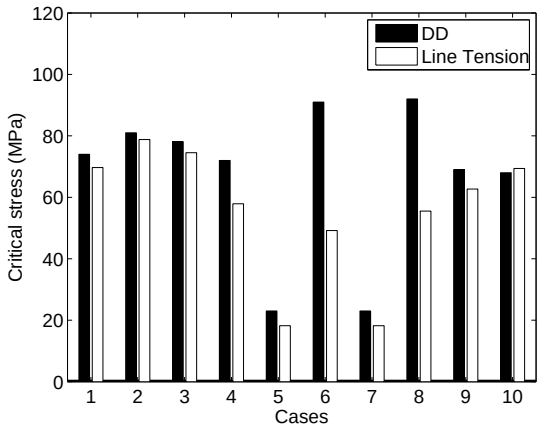

(b) Anisotropic

Fig. 4. Calculated critical stress for the different initial conditions of Table 1 ($L = 1000\, a_0$). (a) Critical stress comparison between full anisotropic elasticity and the Reuss and Voigt isotropic averages. (b) Comparison between the analytical anisotropic line tension model and the full anisotropic DD method.

features are noteworthy: i) the $\boldsymbol{b} = [100]$ cases have a fairly uniform critical stress across cases 1–4. This is due to the fact that the lowest energy orientation is a mixed configuration, and so the stress required to operate source does not depend strongly on the initial segment orientation, since the sharp corners permitted at this level of anisotropy allow the source to expand by generating dislocation line in this direction only. This is borne out by the additional mixed cases 9 and 10, which have very similar critical stresses, and show that for the $\boldsymbol{b} = [100]$ cases, the initial orientation is largely inconsequential. ii) The opposite is true for the $\boldsymbol{b} = \frac{1}{2}[111]$ cases, where a large energy difference exists between edge and screw, and the corners which appear do not allow the source to circumvent the screw-edge asymmetry. When the initial segment is pinned in a screw orientation (6,8), the source has no choice but to generate at least some energetically-costly edge segments, requiring a much greater stress

than the initially-edge case, where screw arms can be extended very easily. iii) Comparing the anisotropic results with the isotropic ones in Fig. 4(a), we find a lower critical stress on average than for the Voigt averages, and a higher one on average than for the Reuss averages. This is consistent with the fact that Voigt averages in general overestimate characteristic stresses and Reuss averages underestimate them. The analytical line tension results are determined using the method of Refs.[8, 15], and contain some arbitrariness in the choice of the integration cutoffs (we use a_0 for the inner cutoff and $1000a_0$ for the outer, which are the only lengthscales in the problem). This arbitrariness enters only logarithmically and the results are in excellent agreement, with the exception of cases 6 and 8. The differences in these cases can be attributed to the choice of criterion for yield: in the line tension model, the critical stress is defined as the stress at which the Frank-Read source bows into a shape that is exactly half of the equilibrium shear loop. In other words, the line tension model predicts the half-loop to be the critical configuration for Frank-Read source activation [15]. Whilst this is adequate for some cases, the more realistic criterion we use for the numerical calculations (*i.e.* the stress above which no stable configuration exists) demonstrates that in some cases, the dislocation can remain stable even when it has already gone beyond the half-loop configuration, due to the long range elastic interactions not captured in the line tension model.n. This is clear from cases 6 and 8 in Fig. 3.

Previous work from the same authors [10] has studied the equilibrium shape of dislocation shear loops in anisotropic elasticity and has computed their energy as a function of orientations, loop radius and temperature. Although the equilibrium shapes exhibit cornered shapes similar to those observed in the Frank-Read sources, the critical stress value cannot be deduced from the equilibrium shear loop shape calculations. There is no obvious relation between the energy of a loop, given in Ref. [10] and the critical stress obtained in Fig. 4. The energy of a loop averages the screw and the edge components of the Frank-Read sources and is almost constant for a given Burgers vector. In our calculations, the critical stress is strongly dependent on the initial orientation of the Frank-Read segment.

4 Conclusions

FR sources are amongst the most important microstructural features of metals, and their properties play a large rôle in governing mechanical behavior such as yield and plastic flow. Our simulations demonstrate the importance of including elastic anisotropy when modeling high temperature iron, and since the anisotropic behavior can be traced back to the proximity of the $\alpha - \gamma$ transition, the results will also apply to a greater or lesser degree to ferritic steels. The stress required to operate an FR source is strongly dependent on its Burg-

ers' vector and orientation, and in particular those orientations which provide plastic displacement by extending $\boldsymbol{b} = \frac{1}{2}[111]$ screw segments can operate at very low applied stresses when the elastic anisotropy is significant. This could offer a possible explanation for the well known loss of strength suffered by iron and ferritic steels as the $\alpha - \gamma$ transition temperature is approached (see [12, 13] and references therein). In addition to these quantitative differences, striking sharp-cornered configurations arose in the simulations, particularly noticeable in the $\boldsymbol{b} = [100]$ cases, in agreement with recent analytical results, and transmission electron microscope observations [16], concerning the instability of certain dislocation orientations at high anisotropy. None of these effects can be captured by any isotropic approximation in three dimensions, since the limitation to two independent moduli allow only the overall stress scale (set by μ) and the edge-screw energy difference (set by ν) to be adjusted.

Acknowledgments

The authors thank Prof D.M. Barnett for countless stimulating discussions and helpful suggestions, and Mr J. Yin for collaboration during work on Ref.[11]. S. Aubry is supported by the Army High Performance Computing Research Center at Stanford. This work was partly funded by the European Communities under the Contracts of Association between EURATOM and CCFE, and was carried out within the framework of European Fusion Development Agreement. The views and opinions expressed herein do not necessarily reflect those of the European Commission. Work at CCFE was partially funded by the RCUK Energy Programme under Grant No. EP/I501045. This work performed under the auspices of the U.S. Department of Energy by Lawrence Livermore National Laboratory under Contract DE-AC52-07NA27344.

References

[1] J.P. Hirth and J. Lothe. Theory of Dislocations. *John Wiley and Sons, Inc., 1982,*, page 857, 1982.

[2] W. Cai and V.V. Bulatov. Computer Simulations of Dislocations, 2006.

[3] B. Devincre and LP Kubin. Mesoscopic simulations of dislocations and plasticity. *Mat. Sci. Eng. A*, 234:8–14, 1997.

[4] X. Han, N.M. Ghoniem, and Z. Wang. Parametric dislocation dynamics of anisotropic crystals. *Philos. Mag.*, 83(31):3705–3721, 2003.

[5] D.J. Dever. Temperature-dependence of the elastic constants in α-iron single crystals: relationship to spin order and diffusion anomalies. *J. Appl. Phys.*, 43(8):3293, 1972.

[6] F.C. Frank and W.T. Read. Multiplication processes for slow moving dislocations. *Phys. Rev.*, 79:722–723, 1950.

[7] S.P. Fitzgerald and Z. Yao. Shape of prismatic dislocation loops in anisotropic α-Fe. *Philos. Mag. Lett.*, 89(9):581–588, 2009.

[8] S.P. Fitzgerald. Frank–Read sources and the yield of anisotropic cubic crystals. *Philos. Mag. Lett.*, 90(3):209–218, 2010.

[9] A. Arsenlis, W. Cai, M. Tang, M. Rhee, T. Oppelstrup, G. Hommes, TG Pierce, and VV Bulatov. Enabling strain hardening simulations with dislocation dynamics. *Mod. Simul. Mat. Sci. Eng.*, 15:553–595, 2007.

[10] S. Aubry, S.P. Fitzgerald, S.L. Dudarev, and W. Cai. Equilibrium Shape of Dislocation Shear Loops in Anisotropic α-Fe. *Mod. Simul. Mater. Sci. Eng.*, 19:065006–065020, 2011.

[11] J. Yin, D.M. Barnett, and W. Cai. Efficient Computation of Forces on Dislocation Segments in Anisotropic Elasticity. *Mod. Simul. Mat. Sci. Eng.*, 18:045013, 2010.

[12] S.P. Fitzgerald and S.L. Dudarev. Dislocation pile-ups in Fe at high temperature. *Proc. R. Soc. London A*, 464:2549–2559, 2008.

[13] S.P. Fitzgerald and S.L. Dudarev. Interaction between dislocations in bcc iron at high temperature. *J. Nucl. Mat.*, 386:67–70, 2009.

[14] S.P. Fitzgerald and S. Aubry. Self force on dislocation segments in anisotropic crystals. *J. Phys. Condensed Matter*, 22:295403, 2010.

[15] I. Kovacs. The critical shear stress needed for the operation of a dislocation segment as a frankread source in anisotropic crystals. *Phys. Status Solidi*, 3:140, 1963.

[16] J.-L. Boutard, S. Dudarev, and M. Rieth. Modelling structural and plasma facing materials for fusion power plants: Recent advances and outstanding issues in the EURATOM fusion materials programme. *J. Nucl. Mat.*, 417(1-3):1042 – 1049, 2011. Proceedings of ICFRM-14.